DOI: 10.1002/chem.200600977

Controlling Hydrothermal Synthesis

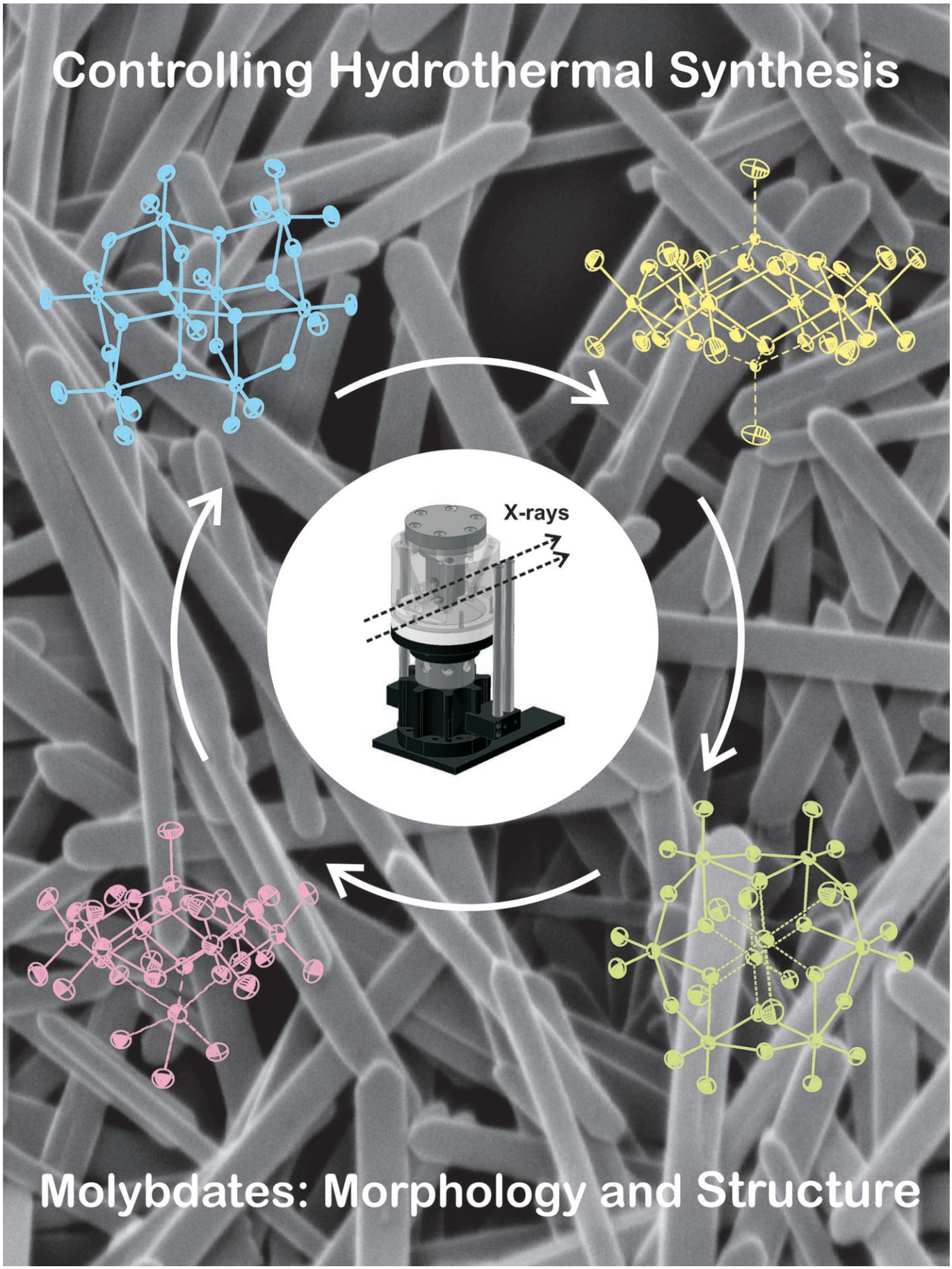

Molybdates: Morphology and Structure

Hydrothermal Synthesis of Molybdenum Oxide Based Materials: Strategy and Structural Chemistry

Alexej Michailovski and Greta R. Patzke*[a]

Abstract: The preparative flexibility of hydrothermal syntheses needs to be systemised for exploring complex structure–synthesis relationships and morphology control options in materials chemistry. This is demonstrated for the targeted hydrothermal preparation of molybdenum oxide materials: firstly, in situ studies were employed for the efficient production of MoO_3 nanofibres. Furthermore, ionic substances as structure-directing tools brought forward a new class of fluorinated polyoxomolybdates.

Keywords: hydrothermal synthesis · in situ spectroscopy · molybdenum oxide · nanostructures · polyoxometalates

Introduction

The current developments in nanotechnology and materials chemistry have also raised high expectations in the field of inorganic synthesis.[1] For the preparation of nano- and mesoporous compounds and composite materials,[2] not only the primary structure of their "building block"[3] units has to be controlled, but they also have to be arranged into a secondary structure, followed by accessing the desired resulting morphology (tertiary structure).[4] Such stepwise assemblies pave the way to the tailoring and functionalisation of highly flexible materials for specific applications.[5] Transition-metal oxides play an important role in this process due to their exceptional variety of important applications, for example, in catalysis, battery technology or photochemistry.[6] The wide spectrum of molybdenum oxide based compounds with its manifold structural motifs and properties has attracted considerable interest in modern materials research.[7,8] MoO_3 already exhibits excellent catalytic,[9] field emission[10] and sensor properties.[11] Its key structural motif, the MoO_6 octahedron, is a versatile building block that gives rise to the large family of polyoxomolybdates.[12] These cluster molecules cover an exceptionally wide range of metal ions assembled into a single molecule (from 3 to 368).[13] Recently, the excellent options for integrating polyoxometalates (POMs) into nanosystems have been pointed out.[14] Furthermore, their important properties include catalytic activity, reversible redox behaviour, ionic conductivity, photochemical processes and antiviral/antibacterial activity.[15] A survey of the wide spectrum of POM-based research areas is given in Table 1.[16–31] POMs are currently employed in host–guest chemistry, and they provide a basis for the creation of large-

Table 1. Selection of current topics in polyoxomolybdate research.

Main topic	Specific feature	Ref.
general synthesis and applications of POMs		
	perspectives of POM research	[16]
	structural chemistry, properties and applications	[12]
	history and future of POM-based chemistry	[17]
	"chimie douce" synthesis of polyoxovanadates	[18]
	POMs: progress in synthesis and catalysis	[19]
	molybdenum oxide based hybrid materials	[20]
catalysis with POMs		
	selective oxidation of hydrocarbons	[21]
	POM-catalysed epoxidation of olefins	[22]
	catalysis with Wells-Dawson heteropoly-compounds	[23]
POM-based magnetic materials		
	magnetic clusters and molecular materials	[24]
	magnetic clusters from polyoxometalate complexes	[25]
other POM-based materials		
	monograph: materials chemistry of POMs	[15a]
	functional polyoxometalate thin films	[26]
	POM-based molecular materials	[27]
	photochromism of hybrid materials based on POMs	[28]
bioactivity of POMs		
	progress in the bioactivity of POMs	[15b]
	antibacterial activity of polyoxotungstates	[29]
modelling of POM systems		
	ab initio modelling of POM structures	[30]
	modelling: electronic and magnetic properties	[31]

[a] Dipl.-Chem. A. Michailovski, Dr. G. R. Patzke
Department of Chemistry and Applied Biosciences
ETH Zürich, Wolfgang-Pauli-Str. 10, 8093 Zürich (Switzerland)
Fax: (+41) 44-632-1149
E-mail: patzke@inorg.chem.ethz.ch

scale architectures.[32] Nevertheless, the majority of POMs are still generated through "one-pot" reactions so that their preparation may depend to a certain extent on "chemical serendipity".[33] As a consequence, highly flexible synthetic techniques are required to organise the growing family of POMs into a preparative "toolbox".[34] For this purpose, the versatility of solvo-/hydrothermal methods is perfectly adequate. They represent a key technique in modern materials synthesis, and they are continuously advanced and refined through their combination with other techniques (e.g. microwave–hydrothermal or electrochemical–hydrothermal).[35] As outlined above, the directed synthesis of transition-metal oxide based materials poses a major preparative challenge in current materials research and nanotechnology, and Table 2 illustrates the vital importance of hydrothermal methods in this context.[36–55] The investigation of the individual hydrothermal reaction pathways, however, is a demanding task that requires the development of highly sophisticated in situ techniques.[56] As a result, hydrothermal processes are still widely operated in the sense of a "black box". Thus, their major advantage—the almost infinite variety of experimental parameters and setups—may turn into a drawback when targeted and predictive syntheses are to be developed.[57] In the following, shape- and structure-control options in hydrothermal synthesis are illustrated for recent examples from the fields of molybdenum oxide based nanoparticles and new fluorinated polyoxomolybdates. Two different approaches to open the "black box" of hydrothermal reactions are compared. Firstly, they can be investigated from the "bottom-up" through the in situ monitoring of their reaction kinetics and the elucidation of reaction mechanisms. Alternatively, they can be systemised through empirical "top-down" strategies based on the strategic evaluation of data collected from hydrothermal field studies[58] or high-throughput experiments.[59]

Table 2. Recent developments in the hydrothermal synthesis of oxide-based materials

Main topic	Specific feature	Ref.
synthesis of nanoparticles		
	general synthesis of nanorods and nanowires	[36]
	inorganic nanorods and nanowires	[37]
	morphology control of vanadium oxide materials	[38]
	multicomponent oxide nanowires	[39]
	1D nanostructures of transition metal oxides	[40]
	oxide and chalkogenide nanoparticles	[41]
	magnetic nanoparticles	[42]
synthesis of open-framework and hybrid materials		
	organically-templated metal sulfates and selenates	[43]
	organic–inorganic vanadium oxide architectures	[44]
	development of microporous solids	[45]
hydrothermal synthesis of zeolites		
	nanozeolites: mechanisms and applications	[46]
	characterisation and crystallisation mechanisms	[47]
hydrothermal process development		
	large-scale synthesis of nanoparticles	[48]
	nanomaterials and supercritical fluids	[49]
	supercritical fluids: synthesis of fine particles	[50]
	microwave-hydrothermal morphology control	[51]
	microwave synthesis of nanoporous materials	[52]
	metastable oxide materials through chimie douce	[53]
in situ investigation of hydrothermal reactions		
	recent developments: in situ powder diffraction	[54]
	in situ investigation of zeolite crystallisation	[55]

Control Options in Hydrothermal Synthesis

The ongoing difficulties in the rational planning of inorganic syntheses are a major roadblock on the way to materials design.[33] The above-mentioned alternative strategies of controlling hydrothermal reactions ("bottom-up" vs. "top-down") reflect the general parting of the pathways through the "energy landscape" of inorganic systems: theoretical methods or high-throughput explorations?[33] At first glance, the empirical approach appears to be more straightforward and faster than the complicated task of setting up theoretical models. A closer look at the efficiency of high-throughput methods, however, quickly reveals that they may not be sufficient to fully embrace the complexity of ternary and higher chemical systems: even with a reasonably contained set of starting parameters and a fairly optimistic throughput rate, the complete screening of the Y/Ba/Cu/O-system, for example, would take about 27000 years,[33] whilst the $YBa_2Cu_3O_{7-x}$ superconductors were discovered only approximately 60 years after their parent perovskite compounds.[60] Returning to hydrothermal reactions, this example illustrates that the mere combinatorial screening of the reaction parameters should always be backed up by in situ methods to analyse the complexity of the reaction sequences proceeding in a closed autoclave system. As an alternative control approach, a wide range of additive substances has been made available to steer the assembly of structural building blocks into a defined morphology on the nanoscale.[61,62] The term "additives" in the strict sense of the word refers to substances that adhere to specific crystal facets of a growing particle, thereby altering the relative growth rates of the different facets.[63] This provides a flexible access to the resulting particle shape and aspect ratio. However, many seemingly "inert" additives are also capable of side reactions with the substrate material, such as redox- or intercalation processes. The latent reactivity of these auxiliary substances can be employed in a constructive fashion by turning them into "spacers" (e.g., ionic compounds or large organic molecules) that can be deliberately used for the assembly of structural building blocks, such as POMs, into a defined two-dimensional structure.[64] This will be demonstrated below for the systematic access to new fluorinated polyoxomolybdate types through the use of such "hydrothermal tools": they can both address the primary structure of the POM anion and fine-tune its secondary packing motif (cf. section on fluoromolybdates).

Mechanisms of Hydrothermal Molybdate Synthesis: Complementary Answers to a Challenging Problem

Although the in situ investigation of hydrothermal processes has recently attracted considerable attention, the reaction mechanisms leading to the entire product spectrum covered by hydrothermal methods are still far from explored.[54,65] Whilst special emphasis has been placed upon the formation mechanisms of nano- and microstructured materials in zeolitic,[66] sulfidic[67] and complex oxide systems,[68] relatively little is known about the respective processes leading to nanoscale binary oxides.[69] However, most of the elucidated hydrothermal pathways to nanoparticles fall into two major mechanistic categories: dissolution–precipitation reactions and solid–solid transformations.[70] The use of complementary methods is essential to distinguish between these alternatives by investigating the complex reaction sequences proceeding under hydrothermal conditions from different angles.[71] Taking the hydrothermal formation of highly anisotropic MoO_3 rods from $MoO_3 \cdot 2H_2O$ in neutral or acidic aqueous media (Figure 1a) as an example,[72] we have combined in situ EXAFS and EDXRD methods into a comprehensive experimental strategy.[73]

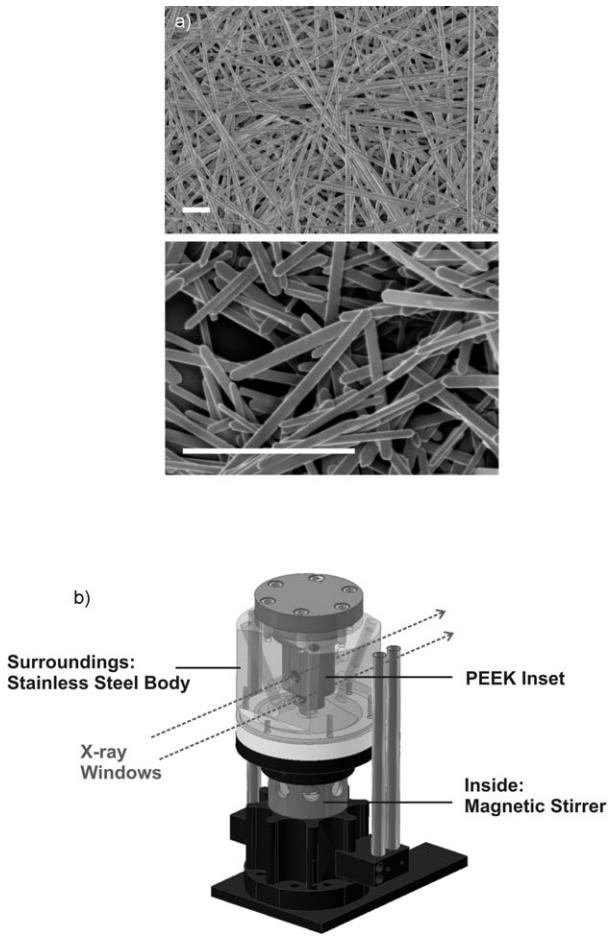

Figure 1. a) Investigation of MoO_3 rod formation (scale bar = 2 μm) with b) a newly constructed in situ EXAFS cell.

EDXRD permits a full characterisation of all crystalline compounds, whilst the EXAFS technique[74] monitors both crystalline and amorphous solid intermediates as well as species in solution.[75] As a consequence, a special in situ EXAFS cell (Figure 1b) was used for the parallel observation of both the solid and the liquid phase during the reaction.[76] Such comprehensive information is vital for proposing a mechanistic hypothesis. The conclusions were subsequently verified by scaled-up laboratory quenching experiments to ensure that they can be applied upon the technical production of MoO_3 fibres.[77] The in situ EXAFS investigation of the temperature-dependent formation of MoO_3 rods revealed that no molybdenum species were present in solution up to 50 °C (Figure 2a).

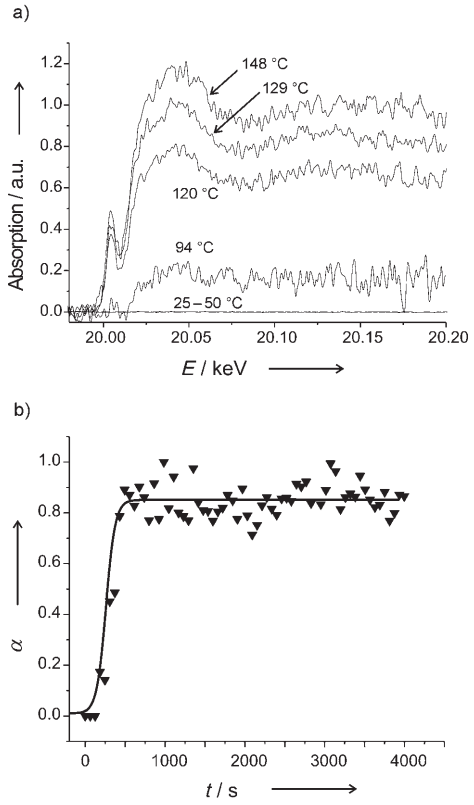

Figure 2. a) Molybdenum K-edge XANES spectra of the liquid phase during the formation of MoO_3 nanorods and b) the time dependence of the extent of reaction α for reflection (021) at 120 °C as determined from in situ EDXRD experiments.

The onset temperature was determined as approximately 100 °C both in the solid and liquid phases of the hydrothermal reaction. The concentration of water-soluble species continues to increase up to 150 °C (Figure 2a). In situ EDXRD experiments revealed the timescale of MoO_3 rod formation at 120 °C in acetic acid (Figure 2b): the crystallisation curve ($\alpha(t)$ vs. time) shows that the reaction is finished within 7–8 min after a short temperature-dependent induc-

tion time of several minutes. This is very quick relative to other solid-state reactions. All in all, the experimental results indicate a rapid dissolution–precipitation mechanism with no crystalline intermediate phases involved. As the presented complementary in situ approach provides comprehensive insight into the different stages of the reaction, this strategy is an effective step towards a more rational hydrothermal materials synthesis. We have recently extended it upon the formation of tungsten oxide based nanomaterials,[78] and further investigations on nanoscale ternary Mo/W oxide systems are in progress.

Structure Control in Hydrothermal Molybdate Synthesis: From Nanomaterials to Crystal Structures

The in situ investigation of the hydrothermal growth of MoO_3 fibres from $MoO_3 \cdot 2H_2O$ (cf. previous section) demonstrates that they are formed through a quite straightforward process involving the dissolution of the educt.[72,77] Consequently, the morphology of the precipitated MoO_3 rods should be controllable through the use of additive substances (cf. section on control options). Starting from this hypothesis, a wide range of potential morphology-directing additives—including biomolecules, organic compounds and inorganic ionic substances—was screened with respect to their influence on the aspect ratio of MoO_3. However, especially the organic additives frequently gave rise to the formation of lamellar composite materials or reduction products under the given hydrothermal conditions (2 d of reaction time at 120–180 °C). Therefore, the preparative efforts were directed to the hydrothermal interaction of Mo^{VI}-based oxidic precursor materials (e.g., MoO_3, molybdic acids or ammonium heptamolybdate) with ionic additives, such as the alkaline earth and alkali halides, which can be classified into three different additive types:[57]

1) Whereas the chlorides and bromides of the lighter alkali cations (Li^+, Na^+) support the hydrothermal formation of MoO_3 rods with nanoscale diameters, they do not significantly change their morphology.
2) The reaction of Mo^{VI}-containing precursor materials with the heavier alkali chlorides or bromides (MX; M = K–Cs; X = Cl, Br) and selected earth alkali halides ($BaBr_2$ and $BaCl_2$) favours the incorporation of the cations into the channels of microcrystalline hexagonal molybdates of the $MMo_5O_{15}OH \cdot 2H_2O$ type.[78]
3) Finally, mm-sized single crystals of polyoxomolybdates with chain- or cluster-containing structural motifs are accessible in the presence of the iodides and fluorides of the heavier alkali cations (K^+–Cs^+).

In the following, ionic additives of the third type are applied as "hydrothermal tools" that systematically address certain polyoxomolybdates and transform them into new fluorinated derivatives. Although the number of molybdenum atoms in polyoxomolybdate clusters may well exceed 300,[13] the structural and synthetic chemistry of the smaller isopolymolybdate anions with $n(Mo) = 4$–10 is still a challenging topic in its own right (Figure 3).[79]

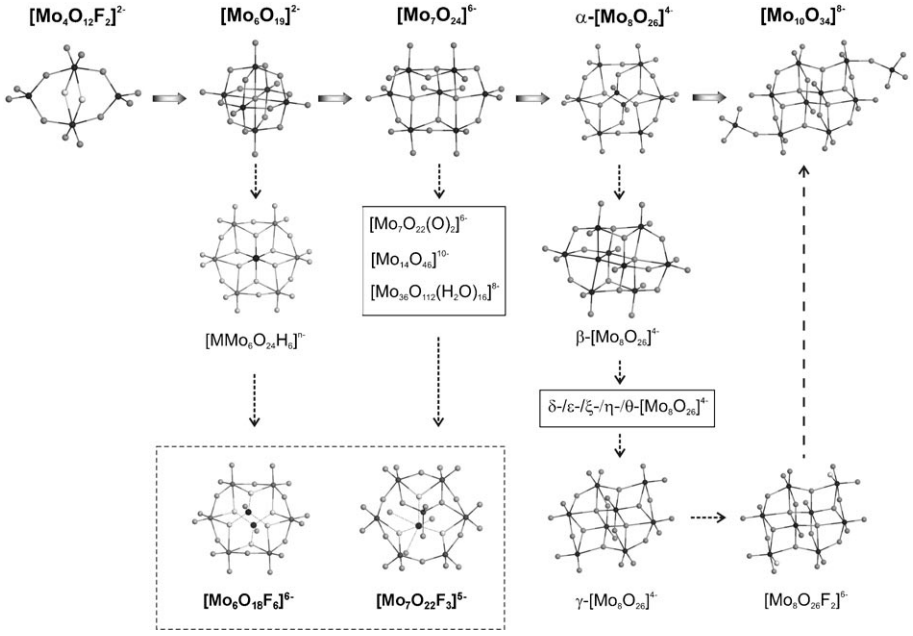

Figure 3. Polyoxomolybdate anions with $n(Mo) = 4$–10 and their new fluorinated derivatives.

Their isomerisation and dimerisation processes have been in the focus of theoretical and preparative studies over the past decades, and they continue to attract current research interest.[80,81] Though they have inspired numerous solvothermal studies,[79] the predictive preparation of a certain molybdate polyanion in combination with a specific cation may still turn into a demanding task that requires considerable experimental experience and intuition.

We have widely investigated the complex hydrothermal structure–synthesis relationships among binary and ternary alkali polyoxomolybdates containing potassium, rubidium and caesium. Two key results brought us to devise an extensive field study:[82]

1) After a series of unsuccessful synthesis attempts based on solid-state methods, the triclinic modification of

$Cs_2Mo_4O_{13}$ had long been considered as nonexistent. This was ascribed to a postulated size mismatch between the large Cs^+ ion and the $[Mo_4O_{13}]^{2-}$ chains.[83] However, our hydrothermal experiments have now brought forward the long sought-after triclinic $Cs_2Mo_4O_{13}$.[84,85] In addition, the hydrothermal reaction of Mo^{VI}-precursor materials with specific alkali iodide combinations afforded new alkali trimolybdates of the $(M/M')Mo_3O_{10}$ type ($M = Rb$; $M' = K$, Cs).[86]

2) The hydrothermal treatment of Mo^{VI}-based starting materials in aqueous MF (M = K–Cs) solutions is a convenient preparative short-cut to highly fluorinated molybdates with structural motifs based on isolated octahedral moieties or on their connection into dimers or chains, respectively. Their preparation is facilitated with respect to conventional high-temperature methods, because the hydrothermal syntheses proceed under mild conditions (temperatures of 220 °C and below and no need for hydrogen fluoride).[82] Furthermore, a multitude of alkali difluorooctamolybdates of the $M_6Mo_8O_{26}F_2{\cdot}nH_2O$ type (M = K–Cs) is readily available from this synthetic pathway through control of the reaction conditions.

Up to now, little is known about the structural chemistry of fluorinated POMs: apart from $[Mo_4O_{12}F_2]^{2-}$,[87] the difluorooctamolybdate ion $[Mo_8O_{26}F_2]^{6-}$ has only been the second fully characterised fluorinated polyoxomolybdate anion with $K_6Mo_8O_{26}F_2{\cdot}6H_2O$ as its single representative (Figure 3).[88] The triclinic $M_2Mo_4O_{13}$ tetramolybdates[83] and the $M_6Mo_8O_{26}F_2{\cdot}nH_2O$-type alkali difluorooctamolybdates (M = K–Cs)[82,88] are structurally closely related (Figure 4):

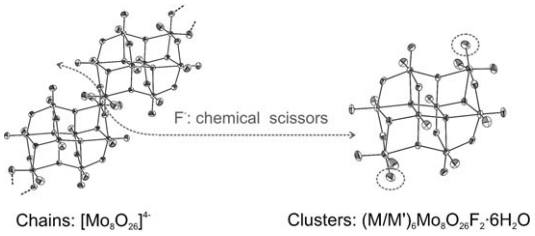

Figure 4. Fluorine anions acting as "chemical scissors" through the decomposition of $M_2Mo_4O_{13}$ alkali tetramolybdates into cluster-containing difluorooctamolybdates.

when the hydrothermal synthesis temperature is raised from 180 °C to 220 °C, the $[Mo_4O_{13}]^{2-}$ chain is cut up into discrete $[Mo_8O_{26}F_2]^{6-}$ units.

Thus, the fluoride anion acts as a "chemical scissors".[82] The structure-directing effect of the alkali cations upon their polyoxomolybdate surroundings is evident from chain-containing molybdates (e.g., the $M_2Mo_3O_{10}{\cdot}nH_2O$ trimolybdates containing infinite $[Mo_3O_{10}]^{2-}$ chains) and cluster-based compounds. Table 3 illustrates how the size of the alkali cation influences both the content of crystal water and the resulting crystal structure in tri-, hepta- and difluorooctamolybdates as representative examples. Consequently, two

Table 3. Structure-directing influence of the alkali cations in binary polyoxomolybdates.

Molybdate type	*n*/space group				
	Li	Na	K	Rb	Cs
$M_2Mo_3O_{10}{\cdot}nH_2O$[109]	5.7	3	3	1	1
	Pn or *P2/n*	*C2m*	*Cmcm*	*Pnma*	*Pnma*
$M_6Mo_7O_{24}{\cdot}nH_2O$[110]	–	14	4	4	7
		$P2_1ab$	$P2_1/c$	$P2_1/c$	$P\bar{1}$
$M_6Mo_8O_{26}F_2{\cdot}nH_2O$[82,88]	–	–	6	6	4–5
			$P\bar{1}$	$P\bar{1}$	$P2_1/c$

different types of "hydrothermal tools" are now available: whereas the fluoride scissors can modify the primary structure of the polyoxomolybdate anion, the combination of two different alkali cations is capable of directing its arrangement into the secondary structure.[82]

From the theoretical point of view, we have investigated the detailed templating effect of the alkali cations on the polyoxomolybdate framework in terms of electrostatic calculations.[89,90] For preparative purposes, high-throughput hydrothermal experiments provide an efficient pre-screening of a given alkali halide/Mo-precursor system for new structural motifs.[82]

The Way to New Fluoromolybdates: Cations as Templating Hydrothermal Tools

In the following section, the systematic application of fluoride anions and alkali/organic cations as structural auxiliaries on the way to new polyoxofluoromolybdates is demonstrated in a step-by-step approach (Figure 5).[82,85]

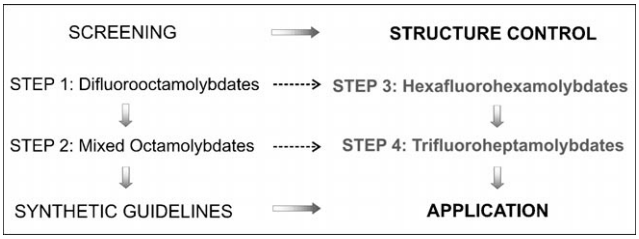

Figure 5. Overview of the research strategy towards new fluorinated polyoxomolybdates.

Step 1—mixed difluorooctamolybdates: Mixed $(M/M')Mo_8O_{26}F_2{\cdot}nH_2O$ (M = K–Cs) alkali difluorooctamolybdates are accessible from the hydrothermal treatment of molybdenum oxide based precursors (e.g., MoO_3, $MoO_3{\cdot}2H_2O$ or ammonium heptamolybdate) in aqueous $(M/M')F$ solutions in the temperature range between 180 and 220 °C (Figure 5, Step 1). The packing motifs of the $[Mo_8O_{26}F_2]^{6-}$ polyanion are controlled by the M/M′ cation combination, and the resulting difluorooctamolybdates can be differentiated into four types (Figure 6). Their structural features are controlled by the size ratio of the alkali cations.

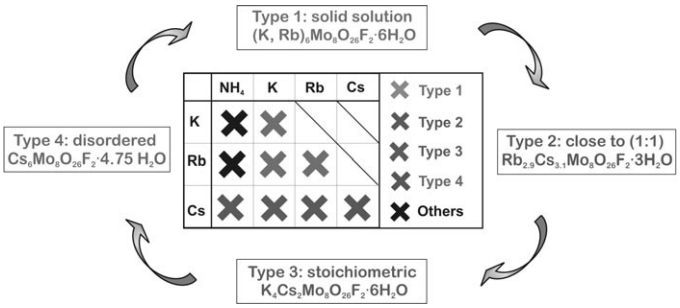

Figure 6. The templating influence of the alkali cations on the crystal structure of mixed difluorooctamolybdates leads to four different $(M/M')Mo_8O_{26}F_2{\cdot}nH_2O$ types.

- **Type 1**: The triclinic type 1 difluorooctamolybdates are formed in the KF/RbF/MoO_3 hydrothermal system as a continuous solid solution series of $K_xRb_{6-x}Mo_8O_{26}F_2{\cdot}6H_2O$ $(0<x<6)$ compounds. Despite their complete miscibility, however, the cations are not statistically distributed among the three different crystallographic sites—they exhibit distinct site preferences instead.
- **Type 2**: This trend is continued among the monoclinic type 2 $M_xCs_{6-x}Mo_8O_{26}F_2{\cdot}3H_2O$ difluorooctamolybdates ($M=Rb$, NH_4; $x\approx3$). The packing motif of the $[Mo_8O_{26}F_2]^{6-}$ polyanions differs from the type 1 series. The miscibility of the cations is furthermore restricted, giving rise to 1:1 compounds with a very narrow phase width. As a result, the cationic site preferences are even more pronounced compared to the type 1 difluorooctamolybdates.
- **Type 3**: $K_4Cs_2Mo_8O_{26}F_2{\cdot}6H_2O$ is the only representative of the type 3 difluorooctamolybdates with a monoclinic structure based on a third packing motif of the $[Mo_8O_{26}F_2]^{6-}$ ions. The miscibility and site occupancy trends among the cations are continued: $K_4Cs_2Mo_8O_{26}F_2{\cdot}6H_2O$ displays no more significant phase width, and the K and Cs cations occupy separate sites.
- **Type 4**: The Cs-rich $M_xCs_{6-x}Mo_8O_{26}F_2{\cdot}3H_2O$ difluorooctamolybdates ($M=K$, Rb; $x<1$) exhibit a heavily disordered structure that can be interpreted as the superposition of two polyanion packing motifs in a 90:10 ratio. As has been outlined above for the case of t-$Cs_2Mo_4O_{13}$,[82] the interaction of the sterically demanding Cs^+ ions with the polyoxomolybdate environment tends to get complicated.

These structure–synthesis relationships among mixed alkali difluorooctamolybdates can be summed up into a synthetic guideline: To exert a significant structure-directing effect on polyoxomolybdate clusters, a pair of countercations with a size difference should be used.

Step 2—packing motifs among β-octamolybdates: This "rule-of-thumb" was verified for a series of octamolybdates containing the β-$[Mo_8O_{26}]^{4-}$ ion[91] (cf. Figure 3) in combination with alkali cations and larger organic cations (Figure 5, Step 2). As discussed further above in the section on additives, the choice of the organic cation is crucial: the presence of long aliphatic chains, for example, may favour the formation of layered intercalation compounds over POMs. Even cations of medium size, such as tetraethylammonium (NEt_4), frequently give rise to structural disorder in the resulting organic/inorganic POMs. Thus, we have opted for 1-azonia-spiro[4.4]nonane[92] (hereafter denoted "asn") as a compact, bicyclic cation (Figure 7). The β-octamolybdates

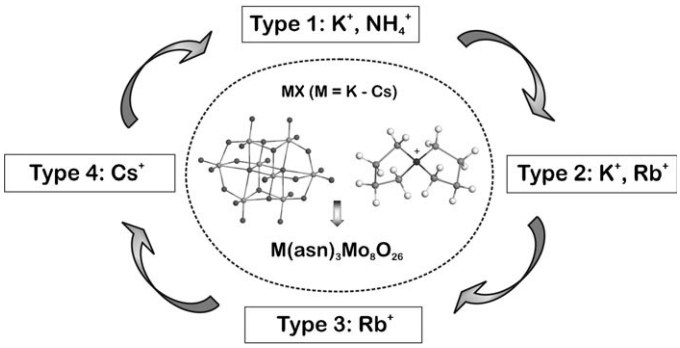

Figure 7. The structure-directing influence of alkali cations in mixed organic/inorganic β-octamolybdates generates four different $M(asn)_3Mo_8O_{26}$ types.

obtained from the MBr/asnBr/MoO_3 ($M=NH_4$, K–Cs) hydrothermal systems at 180 °C were all of the β-$M(asn)_3Mo_8O_{26}$ type (Figure 7). The presence of an alkali cation in the structure alters the packing motif of the β-$[Mo_8O_{26}]^{4-}$ ions with respect to the parent compound β-$(asn)_4Mo_8O_{26}$. Furthermore, four different packing motifs could be obtained among the β-$M(asn)_3Mo_8O_{26}$ ($M=NH_4$, K–Cs) series, depending on the alkali cation. This result indicates that the templating effect of cation pairs with a size difference might be of more general use to systemise the hydrothermal search for new structural motifs among POMs.

Step 3—systematic ways to new hexafluorohexamolybdates: To apply the aforementioned synthetic trend ("templating with asymmetric cation pairs") on the formation of new fluorinated polyoxomolybdates, extensive screening experiments were performed in the MF/CsF/MoO_3 and MF/CsF/$MoO_3{\cdot}2H_2O$ ($M=Li$, Na, K) hydrothermal systems (Figure 5, Step 3). This led to the formation of the new $(M/M')_6Mo_6O_{18}F_6{\cdot}nH_2O$ ($M=Na$, Li; $M'=K$–Cs, NH_4) hexafluorohexamolybdates, which are formed within rather narrow synthetic parameter windows, for example, carefully adjusted MF/M′F-ratios at a reaction temperature of 220 °C. All hexafluorohexamolybdates have the $[Mo_6O_{18}F_6]^{6-}$ anion with idealised D_{3d} symmetry in common (Figures 8 and 10 below).[89]

The hexafluorohexamolybdate anion bears close resemblance to the Anderson–Evans type[93] hexamolybdates ($[H_6MMo_6O_{24}]^{n-}$ $M=Al$, Cr, Zn, Cu, Co, Ni, Pt…).[94]

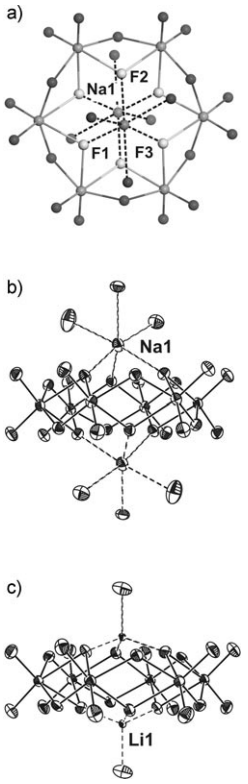

Figure 8. Structure of the ring-shaped $[Mo_8O_{16}F_6]^{6-}$ fluoromolybdate moiety in a,b) $Na_2Cs_4Mo_6O_{18}F_6{\cdot}6H_2O$ and c) $Li_2Cs_4Mo_6O_{18}F_6{\cdot}6H_2O$.

Though the Anderson–Evans cluster motif continues to attract research interest since its discovery 70 years ago,[93] its heteroatom-free variation, the hypothetical planar $[H_6Mo_6O_{24}]^{6-}$ ion, has never been reported. Instead, the compact $[Mo_6O_{19}]^{2-}$ ion (Lindqvist type) represents the energetically favourable arrangement of six MoO_6 octahedra into a polyanion (Figure 3).[95] The $[Mo_6O_{18}F_6]^{6-}$ anion can be thus be regarded as the first "cored" derivative of the Anderson–Evans cluster. The $(M/M')_6Mo_6O_{18}F_6{\cdot}nH_2O$ compounds can furthermore be subdivided into three types: $Li_2Cs_4Mo_6O_{18}F_6{\cdot}6H_2O$ (type 1) and $Na_2Cs_4Mo_6O_{18}F_6{\cdot}6H_2O$ (type 2) exhibit different packing motifs of the hexafluorohexamolybdate anions (Table 4). Though the $Na_2M_4Mo_6O_{18}F_6{\cdot}nH_2O$ (M = K, Rb, NH_4; type 3) series is structurally closely related to $Na_2Cs_4Mo_6O_{18}F_6{\cdot}6H_2O$ (type 2, Table 4), the crystal growth of these compounds is far more difficult than for types 1 and 2. The crystal structures of the type 1 and 2 hexafluorohexamolybdates illustrate that the combination of a large and a small cation is essential to generate the structural features; whereas the latter stabilises the $[Mo_6O_{18}F_6]^{6-}$ anion through its coordination to the fluorine atoms (cf. Figure 8), the former sustains the packing motif of the ring moieties. These different roles of the cations are furthermore clearly reflected in their large electrostatic potential differences.[89]

Step 4—from hexafluorohexamolybdates to new trifluoroheptamolybdates: As the combined hydrothermal reaction of alkali and organic halides with Mo^{VI}-based precursors exerts a distinct structure-directing effect upon the resulting β-octamolybdates (Figure 7), in the next step the NaF/NMe_4F/MoO_3 hydrothermal system was subjected to an intense search for new fluorinated polyoxomolybdate types (Figure 5, Step 4). As a result, the triclinic and monoclinic modifications of $Na_2(NMe_4)_3Mo_7O_{22}F_3{\cdot}6H_2O$ were obtained (type 5, Table 4).[89] Both compounds have the new $[Mo_7O_{22}F_3]^{5-}$ trifluoroheptamolybdate anion with idealised C_{3v} symmetry in common (Figure 9a).[89]

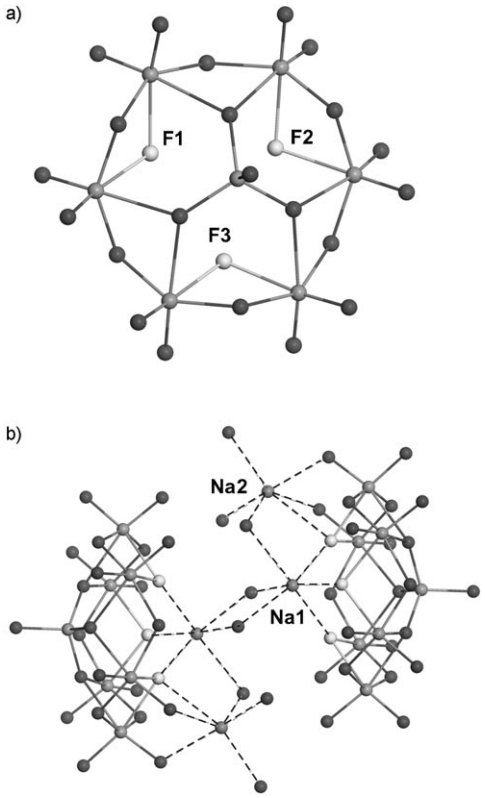

Figure 9. a) The $[Mo_7O_{22}F_3]^{5-}$ anion and b) its interconnection into dimers through sodium cations coordinated to the fluorinated faces of the polyanion.

It can be interpreted as the structural "missing link" between the α-$[Mo_8O_{26}]^{4-}$ ion[96] and the $[Mo_6O_{18}F_6]^{6-}$ hexafluorohexamolybdate ion (Figure 10),[89] because the $[Mo_7O_{22}F_3]^{5-}$ ion contains a hydrophilic, fluorinated face and a hydrophobic face covered by a MoO_4 tetrahedron. This renders it a "Janus head" polyanion, and in both modi-

Table 4. Different structure types of new fluorinated polyoxomolybdates.[89]

Fluoromolybdate	Type	Lattice constants						Space group
		a [Å]	b [Å]	c [Å]	α [°]	β [°]	γ [°]	
$Li_2Cs_4Mo_6O_{18}F_6{\cdot}6H_2O$	1	8.076(1)	10.272(1)	10.417(1)	109.63(1)	92.34(1)	113.04(1)	$P\bar{1}$
$Na_2Cs_4Mo_6O_{18}F_6{\cdot}6H_2O$	2	10.315(1)	9.909(1)	15.702(2)	90.00	106.59(1)	90.00	$P2_1/n$
$Na_2K_4Mo_6O_{18}F_6{\cdot}2H_2O$	3	15.182(1)	9.711(1)	9.811(1)	90.00	107.72(2)	90.00	$P2_1/n$
$0.9\,Na_4(NMe_4)_2Mo_6O_{18}F_6{\cdot}10H_2O{\cdot}$ $0.1\,Na_3(NMe_4)_2Mo_7O_{22}F_3{\cdot}9H_2O$	4	8.166(1)	11.865(1)	11.933(1)	108.35(1)	97.72(1)	109.64(1)	$P\bar{1}$
t-$Na_2(NMe_4)_3Mo_7O_{22}F_3{\cdot}6H_2O$	5	11.763(1)	11.856(1)	17.058(2)	108.66(1)	93.99(1)	106.43(1)	$P\bar{1}$
m-$Na_2(NMe_4)_3Mo_7O_{22}F_3{\cdot}6H_2O$	5	19.141(5)	13.982(3)	32.214(8)	90.00	99.47(1)	90.00	$C2/c$

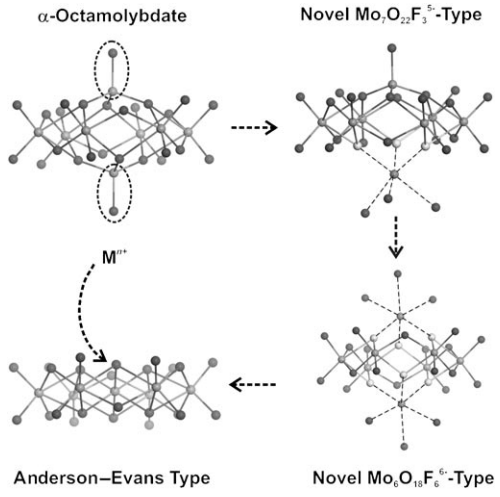

Figure 10. Structural relationships between the α-$[Mo_8O_{26}]^{4-}$ octamolybdate anion, the new $[Mo_7O_{22}F_3]^{5-}$ and $[Mo_6O_{18}F_6]^{6-}$ fluoromolybdates and the Anderson–Evans polyanions of the $[H_6MMo_6O_{24}]^{n-}$ type (clockwise).

fications of $Na_2(NMe_4)_3Mo_7O_{22}F_3{\cdot}6H_2O$ the $[Mo_7O_{22}F_3]^{5-}$ ions are arranged as dimers that are interconnected through Na–F contacts at the fluorinated face, whilst the MoO_4-capped sides are surrounded by the NMe_4^+ ions (Figure 9b).

So the selection of the Na^+/NMe_4^+ ion pair with a considerable difference in size and polarisability led to the formation of another new polyoxofluoromolybdate. Moreover, variations in the hydrothermal conditions (e.g. an increase in the initial fluoride/Mo-precursor molar ratio) gives rise to the formation of a third fluoromolybdate type containing both the trifluoroheptamolybdate and the $[Mo_6O_{18}F_6]^{6-}$ ions: the $(Na_4(NMe_4)_2Mo_8O_{16}F_6{\cdot}10H_2O)_{1-x}(Na_3(NMe_4)_2Mo_7O_{22}F_3{\cdot}9H_2O)_x$ ($0.06 < x < 0.44$) series of the type 4 (Table 4). The $[Mo_7O_{22}F_3]$/$[Mo_6O_{18}F_6]$ ratio increases with the NMe_4F/NaF ratio in the starting material. This trend demonstrates the structural fine-tuning options for size-mismatched cation pairs as hydrothermal tools.

Fine-tuning of organic cations as hydrothermal tools:[85] Generally, the idea of designing the secondary structure of POMs through tailor-made organic cations is an inspiring challenge. As a continuation of our structure-directing hydrothermal synthesis of β-$M(asn)_3Mo_8O_{26}$ (M = K–Cs, NH_4) octamolybdates (Figure 5, Step 2) and $Na_2M_4Mo_6O_{18}F_6{\cdot}6H_2O$ (M = K–Cs, NH_4) hexafluorohexamolybdates (Step 3), the packing motif of the $[Mo_6O_{18}F_6]^{6-}$ moieties in $Na_4(asn)_2Mo_6O_{18}F_6{\cdot}6H_2O$ could furthermore be arranged into layers of polyanions.

They are interconnected through sodium cations and separated by the organic "spacer" cations (Figure 11, middle). When the asn cation is replaced by the *N,N*-dimethylmorpholinium cation[97] (in the following: dmm) in the hydrothermal reaction, $Na_3(dmm)_3Mo_6O_{18}F_6{\cdot}5H_2O$ is formed. Here, the hexafluorohexamolybdate anions are interconnected through the sodium cations into stacks that are kept apart by the dmm cations (Figure 11, top). Note that there are no significant electrostatic interactions between the oxygen atoms of the organic ligand and the sodium cations or the crystal water molecules. In the first place, even extended scans among other organic cation types in combination with the NaF/MoO_3 hydrothermal system did not bring forward any further new trifluoroheptamolybdates apart from the $Na_2(NMe_4)_3Mo_7O_{22}F_3$-based compounds (Figure 5, Step 4). A strategic modification of the organic cation put an end to this "dry spell": the asn ligand was replaced by a derivative containing two additional oxygen atoms (1-azonia-4,4′-dioxaspiro[5.5]undecane;[98] in the following:

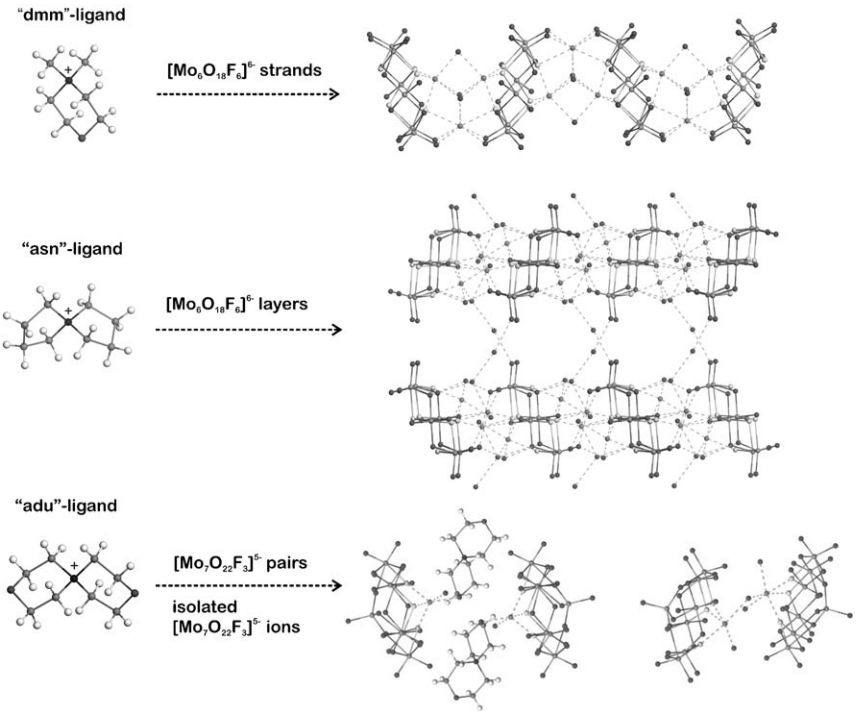

Figure 11. The structure-directing effect of the organic cation on the packing motif of $[Mo_6O_{18}F_6]^{6-}$- and $[Mo_7O_{22}F_3]^{5-}$-type polyoxofluoromolybdates (dmm = N, N-dimethylmorpholinium; asn = 1-azonia-spiro-[4.4]nonane; adu = 1-azonia-4,4′-dioxaspiro[5.5]undecane; the organic cations have been omitted for clarity).

adu, see Figure 11). The resulting increase in polarity with respect to the asn ligand is already reflected by the presence of different packing motifs of the $[Mo_8O_{26}]^{4-}$ ions in the binary β-$M_4Mo_8O_{26}$ (M = asn, adu) octamolybdates. Most importantly, however, $Na(adu)_4Mo_7O_{22}F_3{\cdot}4H_2O$ was obtained as a new representative of the trifluoroheptamolybdate series. The $[Mo_7O_{22}F_3]^{5-}$ ions are arranged into pairs that are stacked along the *c* axis (Figure 11, bottom) in an ABA··· layer sequence, thereby causing its exceptional length of 54.3(1) Å compared to the other new fluorinated POMs (with lengths of the *c* axis up to 32 Å). The stacking motif is composed of the aforementioned "Janus head" dimers (cf. Figures 11 and 8b) and of the first isolated $[Mo_7O_{22}F_3]^{5-}$ ions: their capping sodium cations are coordinated to an oxygen atom of the adu ligand, so that the ring moieties have been isolated for the first time (Figure 11, bottom). In this way, a careful tuning of the organic ligand can be employed to direct the secondary structure of the new fluorinated polyoxomolybdates.

Trends—synthesis of new fluoromolybdates: The outlined systematic quest for new fluorinated polyoxomolybdates is based on an iterative process starting from extensive hydrothermal field studies,[58] followed by the application and the continuous refinement of the emerging synthetic guidelines (Figure 5 and Figure 10). This strategy demonstrates that a combination of chemical intuition and experience with effective screening techniques might be a fast track towards reliable hydrothermal structure–synthesis relationships.[82] Although the influence of "serendipity" is being reduced to a minimum, it must be kept in mind that some of the compounds discussed above are only accessible within strictly confined parameter windows. Thus, the initial hydrothermal screening must be conducted in narrow steps and even the most detailed investigation may leave the chemist with the premonition that some compounds might still have been overlooked. For this reason, theoretical calculations[81] are of key importance in developing a comprehensive "design" approach in the hydrothermal synthesis of Mo-based materials and related compounds. They are especially indispensable to keep track of the ever increasing family of molybdenum-based POMs and the complex structure–synthesis relations among their manifold isomers and derivatives (Figure 3).

Perspectives in Hydrothermal Molybdate Chemistry

Synthetic developments: Although the important role of polyoxomolybdates as connectors between nanostructured materials and the atomic scale is undeniable,[13,14] a fully predictive access to their manifold structural motifs still remains a synthetic challenge. Likewise, the shape-control of molybdate materials on the nanoscale is difficult to premeditate.[99] The preceding sections demonstrated that hydrothermal methods provide the necessary experimental and methodological flexibility to cover a wide spectrum of molybdate chemistry. As their manifold preparative options can either be systemised from the "bottom-up" through in situ techniques or by a "top-down" approach based on targeted parameter studies, both strategies should be combined to fully grasp the complexity of real hydrothermal systems.

Another promising solution is the development of more sophisticated hydrothermal setups beyond the classical autoclaves.[35] Over the last decades, for example, great progress has been achieved in the field of hydrothermal–electrochemical,[100] ammonothermal[101] and microwave–hydrothermal techniques.[102] Especially the last are often superior to conventional reactions due to their accelerated kinetics that provide additional morphology control options and a convenient access to metastable phases.[103] Parallel to the ongoing advancement of autoclave types, new hydrothermal media are currently explored, such as the promising potential of ionic liquids in solvothermal nanomaterials synthesis.[104] Furthermore, the nanoscale structural dimensions of biomolecules have been implemented as templates in "green chemistry" hydrothermal approaches towards anisotropic nanoparticles under mild conditions.[62] This vast arsenal of new preparative perspectives raises aspirations for the discovery of new molybdenum-based materials.

The same applies for the recent breakthroughs in the field of high-throughput hydrothermal synthesis: multiclaves for more than 100 parallel reactions have been constructed, and in the cutting-edge systems, the entire hydrothermal process from the synthesis over the workup to the characterisation is performed continuously without any sample transfers.[59] The efficiency of these methods has been demonstrated for the high-throughput synthesis of zeolitic and open-framework systems, and they would open up new directions in the preparation of nanoscale molybdenum oxides and POMs as well.

Analytical and theoretical approaches: Hydrothermal crystallisation processes can nowadays be monitored in situ with an extraordinary wide spectrum of spectroscopic and imaging (AFM, SEM, TEM, etc.) techniques covering both changes in the long-range order (EDXRD, neutron diffraction, etc.) and in the local structure (XANES, EXAFS, NMR, etc.). The future of these efforts lies in their combination into multitechnique approaches, such as complementary in situ EXAFS/EDXRD (see above) or SAXS/WAXS studies.[56] In this way, many of the hitherto unknown formation mechanisms of POM and molybdenum oxide based nanoparticles might now be uncovered. Current examples are the important family of bismuth molybdates that are just being transferred onto the nanoscale[105,106] or the cutting-edge research area of inorganic–organic composite materials.[8]

From the theoretical point of view, the manifold isomerisation reactions of polyoxomolybdates, namely among the $[Mo_8O_{26}]^{4-}$ octamolybdates, continue to inspire profound theoretical studies. Only recently, hydrothermal methods have brought forward the new θ-octamolybdate isomer.[107] It has been identified as the lowest energy structure through the help of single-point and geometry-optimised energies,

whereas the δ-octamolybdate, which has previously been regarded as the most stable isomer,[108] only appears to represent a local minimum. This interesting breakthrough demonstrates the importance of intense interactions between theoretical chemistry and hydrothermal expertise in the ongoing search for new POM structures.

Conclusion

As outlined above, the hydrothermal synthesis of cutting-edge molybdenum-based nanomaterials and POMs is a fascinating and complex research area and a "melting pot" of interdisciplinary research activities joining in situ methods, combinatorial techniques and experimental structure–synthesis studies. Furthermore, theoretical methods are an essential guide through the "Bermuda Triangle" (structure–synthesis–morphology control) that hydrothermal chemists face on their quest for to the comprehensive design of a new material. Modern hydrothermal molybdate synthesis is now in a unique bridging position to join structural design on the atomic scale (POMs) with the emerging class of composite and nanomaterials. Thus, it is expected to play an important role in the production of polyoxometalate-based integrated nanosystems (PINs).[14] However, there is still a hint of intuition and serendipity attached to each synthetic breakthrough, in spite of all the outlined options for systemising hydrothermal processes. Maybe the perpetual fascination of molybdate chemistry has its source in these last unresolved questions.

Acknowledgements

We thank Prof. Dr. Reinhard Nesper (Laboratory of Inorganic Chemistry, ETH Zürich) for his steady interest and for the continuous support of this work. The EXAFS investigations were performed in cooperation with the group of Prof. Dr. Alfons Baiker and PD Dr. Jan-Dierk Grunwaldt (Institute for Chemical and Bioengineering, ETH Zürich, Switzerland), and we gratefully acknowledge their expertise and support. For the EDXRD studies, we are grateful to the group of Prof. Dr. Wolfgang Bensch (Laboratory of Inorganic Chemistry, University of Kiel, Germany). This work was supported by the ETH Zurich, by the Swiss National Science Foundation (MaNEP—Materials with Novel Electronic Properties), and by the National Research Program "Supramolecular Functional Materials".

[1] a) *The Chemistry of Nanomaterials* (Eds.: C. N. R. Rao, A. Müller, A. K. Cheetham), Wiley-VCH, Weinheim, **2004**; b) *Nanoparticles* (Ed.: G. Schmid), Wiley-VCH, Weinheim, **2004**.
[2] a) C. N. R. Rao, A. K. Cheetham, *J. Mater. Chem.* **2002**, *12*, 2887–2894; b) F. Schüth, *Chem. Mater.* **2001**, *13*, 3184–3195; c) G. Férey, *Chem. Mater.* **2001**, *13*, 3084–3098.
[3] G. Férey, *J. Solid State Chem.* **2000**, *152*, 37–48.
[4] Y. Gong, C. Hu, H. Liang, *Prog. Nat. Sci.* **2005**, *15*, 385–394.
[5] a) R. Tenne, C. N. R. Rao, *Philos. Trans. R. Soc. London Ser. A* **2004**, *362*, 2099–2125; b) G. R. Patzke, F. Krumeich, R. Nesper, *Angew. Chem.* **2002**, *114*, 2554–2571; *Angew. Chem. Int. Ed.* **2002**, *41*, 2446–2461.
[6] C. N. R. Rao, B. Raveau, *Transition Metal Oxides*, Wiley-VCH, Weinheim, **1998**.
[7] N. Guillou, G. Férey, M. S. Whittingham, *J. Mater. Chem.* **1998**, *8*, 2277–2280.
[8] *Perspectives in the Solid State Coordination Chemistry of the Molybdenum Oxides* (Eds.: M. T. Pope, A. Müller), Kluwer Academic, Dordrecht **2001**.
[9] A. Baiker, D. Gasser, *Z. Phys. Chem.* **1986**, *149*, 119–124.
[10] J. Zhou, N. S. Xu, S. Z. Deng, J. Chen, J. C. She, Z. L. Wang, *Adv. Mater.* **2003**, *15*, 1835–1840.
[11] K. M. Sawicka, A. K. Prasad, P. I. Gouma, *Sens. Lett.* **2005**, *3*, 31–35.
[12] a) *Polyoxometalates: From Platonic Solids to Anti-Retroviral Activity* (Eds.: M. T. Pope, A. Müller), Kluwer Academic, Dordrecht **1994**; b) C. L. Hill, *Compr. Coord. Chem. II* **2004**, *4*, 679–759.
[13] "Oxomolybdates: From Structures to Functions in a New Era of Nanochemistry": A. Müller, in *The Chemistry of Nanomaterials* (Eds.: C. N. R. Rao, A. Müller, A. K. Cheetham), Wiley-VCH, Weinheim, **2004**.
[14] D.-L. Long, L. Cronin, *Chem. Eur. J.* **2006**, *12*, 3698–3706.
[15] a) T. Yamase, M. T. Pope, *Polyoxometalate Chemistry for Nanocomposites Design*, Kluwer Academic, Dordrecht, **2002**; b) B. Hasenknopf, *Front. Biosci.* **2005**, *10*, 275–287.
[16] M. T. Pope, A. Müller, *Angew. Chem.* **1991**, *103*, 56–70; *Angew. Chem. Int. Ed. Engl.* **1991**, *30*, 34–48.
[17] P. Gouzerh, M. Che, *Actual. Chim.* **2006**, *298*, 9–22.
[18] J. Livage, *Coord. Chem. Rev.* **1998**, *178–180*, 999–1018.
[19] Y. Gong, C. Hu, H. Liang, *Prog. Nat. Sci.* **2005**, *15*, 385–394.
[20] P. J. Hagrman, D. Hagrman, J. Zubieta, *Angew. Chem.* **1999**, *111*, 2798–2848; *Angew. Chem. Int. Ed.* **1999**, *38*, 2639–2684.
[21] F. Cavani, *Catal. Today* **1998**, *41*, 73–86.
[22] N. Mizuno, K. Yamaguchi, K. Kamata, *Coord. Chem. Rev.* **2005**, *249*, 1944–1956.
[23] L. E. Briand, G. T. Baronetti, H. J. Thomas, *Appl. Catal. A* **2003**, *256*, 37–50.
[24] E. Coronado, C. J. Gómez-García, *Comments Inorg. Chem.* **1995**, *17*, 255–281.
[25] J. M. Clemente-Juan, E. Coronado, *Coord. Chem. Rev.* **1999**, *193–195*, 361–394.
[26] S. Liu, D. Volkmer, D. G. Kuth, *J. Cluster Sci.* **2003**, *14*, 405–419.
[27] E. Coronado, C. J. Gómez-Garcia, *Chem. Rev.* **1998**, *98*, 273–296.
[28] T. He, J. Yao, *Prog. Mater. Sci.* **2006**, *51*, 810–879.
[29] Y. Tajima, *Mini-Rev. Med. Chem.* **2005**, *5*, 255–268.
[30] M.-M. Rohmer, M. Bénard, J.-P. Blaudeau, J.-M. Maestre, J.-M. Poblet, *Coord. Chem. Rev.* **1998**, *178–180*, 1019–1049.
[31] J. M. Poblet, X. López, C. Bo, *Chem. Soc. Rev.* **2003**, *32*, 297–308.
[32] C. Sanchez, G. J. D. A. Soler-Illia, F. Ribot, T. Lalot, C. R. Mayer, V. Cabuil, *Chem. Mater.* **2001**, *13*, 3061–3083.
[33] M. Jansen, *Angew. Chem.* **2002**, *114*, 3896–3917; *Angew. Chem. Int. Ed.* **2002**, *41*, 3746–3766.
[34] M. I. Khan, *J. Solid State Chem.* **2000**, *152*, 105–112.
[35] a) K. Byrappa, M. Yoshimura, *Handbook of Hydrothermal Technology*, Noyes, Park Ridge, NJ, **2001**; b) G. Demazeau, *J. Mater. Chem.* **1999**, *9*, 15–18.
[36] C. N. R. Rao, A. Govindaraj, *Nanotubes and Nanowires*, Royal Society of Chemistry, Cambridge **2005**.
[37] C. N. R. Rao, *Prog. Solid State Chem.* **2003**, *31*, 5–147.
[38] Y. Wang, G. Cao, *Chem. Mater.* **2006**, *18*, 2787–2804.
[39] K. S. Shankar, A. K. Raychaudhuri, *Mater. Sci. Eng. C* **2005**, *25*, 738–751.
[40] X. Wang, Y. Li, *Pure Appl. Chem.* **2006**, *78*, 45–64.
[41] M. Rajamathi, R. Seshadri, *Curr. Opin. Solid State Mater. Sci.* **2002**, *6*, 337–345.
[42] M. A. Willard, L. K. Kurihara, E. E. Carpenter, S. Calvin, V. G. Harris, *Int. Mater. Rev.* **2004**, *49*, 125–170.
[43] C. N. R. Rao, J. N. Behera, M. Dan, *Chem. Soc. Rev.* **2006**, *35*, 375–387.
[44] P. J. Hagrman, R. C. Finn, J. Zubieta, *Solid State Sci.* **2001**, *3*, 745–774.
[45] G. Férey, *Chem. Mater.* **2001**, *13*, 3084–3098.
[46] L. Tosheva, V. P. Valtchev, *Chem. Mater.* **2005**, *17*, 2494–2513.

[47] T. Wakihara, T. Okubo, *Chem. Lett.* **2005**, *34*, 276–281.
[48] O. Masala, R. Seshadri, *Annu. Rev. Mater. Res.* **2004**, *34*, 41–81.
[49] E. Reverchon, R. Adami, *J. Supercrit. Fluids* **2006**, *37*, 1–22.
[50] Y. Hakuta, H. Hayashi, K. Arai, *Curr. Opin. Solid State Mater. Sci.* **2003**, *7*, 341–351.
[51] S.-E. Park, J.-S. Chang, Y. K. Hwang, D. S. Kim, S. H. Jhung, J. S. Hwang, *Catal. Surv. Jpn.* **2004**, *8*, 91–110.
[52] G. A. Tompsett, W. C. Conner, K. S. Yngvesson, *ChemPhysChem* **2006**, *7*, 296–319.
[53] J. Gopalakrishnan, *Chem. Mater.* **1995**, *7*, 1267–1275.
[54] R. I. Walton, D. O'Hare, *Chem. Commun.* **2000**, 2283–2291.
[55] P. Norby, *Curr. Opin. Colloid Interface Sci.* **2006**, *11*, 118–127.
[56] a) A. K. Cheetham, C. F. Mellot, *Chem. Mater.* **1997**, *9*, 2269–2279; b) R. W. Gareth, I. K. Aamir, D. O'Hare, *Struct. Bonding* **2006**, *119*, 161–192.
[57] A. Michailovski, F. Krumeich, G. R. Patzke, *Helv. Chim. Acta* **2004**, *87*, 1029–1047.
[58] P. Behrens, A. Glaue, C. Haggenmüller, G. Schechner, *Solid State Ionics* **1997**, *101*, 255–260.
[59] a) N. Stock, T. Bein, *Angew. Chem.* **2004**, *116*, 767–770; *Angew. Chem. Int. Ed.* **2004**, *43*, 749–752; b) T. P. Caremans, C. E. A. Kirschhock, P. Verlooy, J. S. Paul, P. A. Jacobs, J. A. Martens, *Microporous Mesoporous Mater.* **2006**, *90*, 62–68.
[60] J. G. Bednorz, K. A. Müller, *Z. Phys. B* **1986**, *64*, 189–193.
[61] a) S. Mann, *Angew. Chem.* **2000**, *112*, 3532–3548; *Angew. Chem. Int. Ed.* **2000**, *39*, 3392–3406; b) P. Simon, W. Carrillo-Cabrera, P. Formanek, C. Gobel, D. Geiger, R. Ramlau, H. Tlatlik, J. Buder, R. Kniep, *J. Mater. Chem.* **2004**, *14*, 2218–2224.
[62] F. Gao, Q. Y. Lu, S. Komarneni, *J. Mater. Res.* **2006**, *21*, 343–348.
[63] S. Rajam, S. Mann, *J. Chem. Soc. Chem. Commun.* **1990**, 1789–1791.
[64] a) H. Abbas, A. L. Pickering, D.-L. Long, P. Kögerler, L. Cronin, *Chem. Eur. J.* **2005**, *11*, 1071–1078; b) A. Dolbecq, C. Mellot-Draznieks, P. Mialane, J. Marrot, G. Férey, F. Sécheresse, *Eur. J. Inorg. Chem.* **2005**, 3009–3018.
[65] R. I. Walton, F. Millange, R. I. Smith, T. C. Hansen, D. O'Hare, *J. Am. Chem. Soc.* **2001**, *123*, 12547–12555.
[66] a) R. E. Morris, S. J. Weigel, P. Norby, J. C. Hanson, A. K. Cheetham, *J. Synchrotron Radiat.* **1996**, *3*, 301–304; b) D. Hooper, P. Barnes, J. K. Cockcroft, A. C. Jupe, S. D. M. Jacques, S. P. Bailey, F. Lupo, M. Vickers, M. Hanfland, *Phys. Chem. Chem. Phys.* **2003**, *5*, 4946–4950.
[67] L. Engelke, M. Schaefer, M. Schur, W. Bensch, *Chem. Mater.* **2001**, *13*, 1383–1390.
[68] A. M. Beale, G. Sankar, *Chem. Mater.* **2003**, *15*, 146–153.
[69] F. Lupo, J. K. Cockcroft, P. Barnes, P. Stukas, M. Vickers, C. Norman, H. Bradshaw, *Phys. Chem. Chem. Phys.* **2004**, *6*, 1837–1841.
[70] R. I. Walton, *Chem. Soc. Rev.* **2002**, *31*, 230–238.
[71] O. Kirilenko, F. Girgsdies, R. E. Jentoft, T. Ressler, *Eur. J. Inorg. Chem.* **2005**, 2124–2133.
[72] a) M. Niederberger, F. Krumeich, H.-J. Muhr, M. Müller, R. Nesper, *J. Mater. Chem.* **2001**, *11*, 1941–1945; b) G. R. Patzke, A. Michailovski, F. Krumeich, R. Nesper, J.-D. Grunwaldt, A. Baiker, *Chem. Mater.* **2004**, *16*, 1126–1134.
[73] A. Michailovski, J.-D. Grunwaldt, A. Baiker, R. Kiebach, W. Bensch, G. R. Patzke, *Angew. Chem.* **2005**, *117*, 5787–5792; *Angew. Chem. Int. Ed.* **2005**, *44*, 5643–5647.
[74] J.-D. Grunwaldt, A. Baiker, *Phys. Chem. Chem. Phys.* **2005**, *7*, 3526–3539.
[75] L. Engelke, M. Schaefer, F. Porsch, W. Bensch, *Eur. J. Inorg. Chem.* **2003**, 506–513.
[76] J.-D. Grunwaldt, M. Ramin, M. Rohr, A. Michailovski, G. R. Patzke, A. Baiker, *Rev. Sci. Instrum.* **2005**, *76*, 054104-1–054104-7.
[77] A. Michailovski, F. Krumeich, G. R. Patzke, *Chem. Mater.* **2004**, *16*, 1433–1440.
[78] B. Krebs, I. Paulat-Böschen, *Acta Crystallogr. Sect. B* **1976**, *32*, 1697–1704.
[79] M. T. Pope, *Compr. Coord. Chem. II* **2004**, *4*, 635–678.
[80] W. G. Klemperer, W. Shum, *J. Am. Chem. Soc.* **1976**, *98*, 8291–8293.
[81] A. J. Bridgeman, *J. Phys. Chem. A* **2002**, *106*, 12151–12160.
[82] A. Michailovski, J. B. Willems, N. Stock, G. R. Patzke, *Helv. Chim. Acta* **2005**, *88*, 2479–2501.
[83] B. M. Gatehouse, P. Leverett, *J. Chem. Soc. A* **1971**, 2107–2112.
[84] J. Marrot, J.-M. Savariault, *Acta Crystallogr. Sect. C* **1995**, *51*, 2201–2205.
[85] A. Michailovski, G. R. Patzke, unpublished results.
[86] a) M. Ishaque Khan, Q. Chen, J. Zubieta, *Inorg. Chim. Acta* **1993**, *213*, 325–327; b) N. Guillou, G. Férey, *J. Solid State Chem.* **1997**, *132*, 224–227; c) A. Michailovski, G. R. Patzke, *Z. Anorg. Allg. Chem.*, in press.
[87] E. Burkholder, J. Zubieta, *Inorg. Chim. Acta* **2004**, *357*, 279–284.
[88] B. Kamenar, B. Kaitner, N. Strukan, *Acta Crystallogr. Sect. C* **1990**, *46*, 2249–2251.
[89] A. Michailovski, H. Rüegger, D. Sheptyakov, G. R. Patzke, *Inorg. Chem.* **2006**, *45*, 5641–5652.
[90] a) R. Nesper, G. Roch, B. Neukäter, H.-G. von Schnering, MADKUG, A Program for the Calculation of Lattice Energies, Madelung Factors, and Point Potentials, Universität Münster, ETH Zürich, **1993**; b) F. E. Rohrer, R. Nesper, *J. Solid State Chem.* **1998**, *135*, 194–200.
[91] a) J. Fuchs, I. Knöpnadel, *Z. Kristallogr.* **1982**, *158*, 165–179; b) W. T. A. Harrison, *Acta Crystallogr. Sect. C* **1993**, *49*, 1900–1902.
[92] U. Monkowius, S. Nogai, H. Schmidbaur, *Z. Naturforsch. B* **2004**, *59*, 259–263.
[93] a) J. S. Anderson, *Nature* **1937**, *140*, 850; b) H. T. Evans, Jr., *J. Am. Chem. Soc.* **1948**, *70*, 1291–1292.
[94] Selected examples: a) A. Perloff, *Inorg. Chem.* **1970**, *9*, 2228–2239; b) C. C. Allen, R. C. Burns, G. A. Lawrance, P. Turner, T. W. Hambley, *Acta Crystallogr. Sect. C* **1997**, *53*, 7–9; c) D. Drewes, B. Krebs, *Z. Anorg. Allg. Chem.* **2005**, *631*, 2591–2594.
[95] L. Lindqvist, *Ark. Kemi* **1950**, *2*, 325–341.
[96] a) V. W. Day, M. F. Fredrich, W. G. Klemperer, W. Shum, *J. Am. Chem. Soc.* **1977**, *99*, 952–953; b) R. S. Rarig, J. Zubieta, *Polyhedron* **2003**, *22*, 177–188.
[97] H. Z. Sommer, H. I. Lipp, L. L. Jackson, *J. Org. Chem.* **1971**, *36*, 824–828.
[98] M. M. Movsumsade, P. A. Gurbanov, N. D. Askerov, G. H. Hodjayev, S. M. Movsumsade, *Azerb. Khim. Zh.* **1979**, *3*, 53–58.
[99] a) G. A. Ozin, *Acc. Chem. Res.* **1997**, *30*, 17–27; b) J. Polleux, N. Pinna, M. Antonietti, M. Niederberger, *J. Am. Chem. Soc.* **2005**, *127*, 15595–15601.
[100] M. Yoshimura, S. E. Yoo, M. Hayashi, N. Ishizawa, *Jpn. J. Appl. Phys.* **1989**, *28*, L2007–L2009.
[101] F. Cheng, S. M. Kelly, S. Clark, N. A. Young, S. J. Archibald, J. S. Bradley, F. Lefebvre, *Chem. Mater.* **2005**, *17*, 5594–5602.
[102] S. Komarneni, *Current Sci.* **2003**, *85*, 1730–1734.
[103] B. L. Newalkar, J. Olanrewaju, S. Komarneni, *Chem. Mater.* **2001**, *13*, 552–557.
[104] a) M. Antonietti, D. B. Kuang, B. Smarsly, Y. Zhou, *Angew. Chem.* **2004**, *116*, 5096–5100; *Angew. Chem. Int. Ed.* **2004**, *43*, 4988–4992; b) P. Wang, S. M. Zakeeruddin, P. Comte, I. Exnar, M. Grätzel, *J. Am. Chem. Soc.* **2003**, *125*, 1166–1167.
[105] R. N. Vannier, G. Mairesse, F. Abraham, G. Nowogrocki, *J. Solid State Chem.* **1996**, *122*, 394–406.
[106] J. Yu, A. Kudo, *Chem. Lett.* **2005**, *11*, 1528–1529.
[107] D. G. Allis, E. Burkholder, J. Zubieta, *Polyhedron* **2004**, *23*, 1145–1152.
[108] R. Xi, B. Wang, K. Isobe, T. Nishioka, K. Toriumi, Y. Ozawa, *Inorg. Chem.* **1994**, *33*, 833–836.
[109] $Li_2Mo_3O_{10}\cdot 5.7H_2O$: S. Hodorowicz, *Krist. Tech.* **1978**, *13*, 4–6; $Na_2Mo_3O_{10}\cdot 3H_2O$: W. Lasocha, A. Rafalska-Lasocha, H. Schenk, *Cryst. Res. Technol.* **1997**, *32*, 577–584; $K_2Mo_3O_{10}\cdot 3H_2O$: W. Lasocha, J. Jansen, H. Schenk, *J. Solid State Chem.* **1995**, *115*, 225–228; $Rb_2Mo_3O_{10}\cdot H_2O$: H.-U. Kreusler, A. Förster, J. Fuchs, *Z. Naturforsch B* **1980**, *36*, 242–244; $Cs_2Mo_3O_{10}\cdot H_2O$: S. Hodorowicz, E.

Hodorowicz, S. Sagnowski, W. Surga, *Pol. J. Chem.* **1980**, *54*, 1859–1864 and reference [46].

[110] $Na_6Mo_7O_{24}\cdot 14H_2O$: K. Sjöbom, B. Hedman, *Acta Chem. Scand.* **1973**, *27*, 3673–3691; $K_6Mo_7O_{24}\cdot 4H_2O$/$Rb_6Mo_7O_{24}\cdot 4H_2O$: H. T. Evans, B. M. Gatehouse, P. Leverett, *J. Chem. Soc. Dalton Trans.* **1975**, *6*, 505–514; $Cs_6Mo_7O_{24}\cdot 7H_2O$: U. Kortz, M. T. Pope, *Acta Crystallogr. Sect. C* **1995**, *51*, 1717–1719.

Published online: November 17, 2006

